

# Quadrupole dominance in the light Sn and in the Cd isotopes

A. P. Zuker

Université de Strasbourg, IPHC, CNRS, UMR7178 Strasbourg, France\*

(Dated: December 11, 2021)

**Background:** The  $B(E2 : 2_1^+ \rightarrow 0_1^+)$  of the Sn isotopes for  $N \leq 64$  exhibit enhancements hitherto unexplained. The same is true for all the Cd isotopes.

**Purpose:** To describe the electromagnetic properties of the Sn and Cd isotopes.

**Method:** Shell-model calculations are performed with a minimally renormalized realistic interaction, supplemented by quasi- and pseudo-SU3 symmetries and Nilsson-SU3 self-consistent calculations. Special care is devoted to the monopole part of the Hamiltonian.

**Results:** (1) Shell-model calculations with the neutron effective charge as single free parameter describe well the  $B(E2 : 2_1^+ \rightarrow 0_1^+)$  and  $B(E2 : 4_1^+ \rightarrow 2_1^+)$  rates for  $N \leq 64$  in the Cd and Sn isotopes. The former exhibit weak permanent deformation corroborating the prediction of a pseudo-SU3 symmetry, which remains of heuristic value in the latter, where the pairing force erodes the quadrupole dominance. Calculations in  $10^7$ - and  $10^{10}$ -dimensional spaces exhibit almost identical  $B(E2)$  behavior: A vindication of the shell model. (2) Nilsson-SU3 calculations describe  $B(E2 : 2_1^+ \rightarrow 0_1^+)$  patterns in  $^{112-120}\text{Cd}$  and  $^{116-118}\text{Sn}$  isotopes having sizable quadrupole moment of non-rotational origin denoted as q-vibrations.

**Conclusion:** A radical reexamination of traditional interpretations in the region has been shown to be necessary, in which approximate symmetries involving the quadrupole force and a high quality monopole Hamiltonian play a major role. What emerges is a bumpy but coherent view.

## I. INTRODUCTION

All nuclear species are equal, but some are more equal than others. The tin isotopes deserve pride of place, because  $Z = 50$  is the most resilient of the magic numbers, because they are very numerous, and many of them stable, starting at  $A = 112$ . For these, accurate data have been available for a long time. As

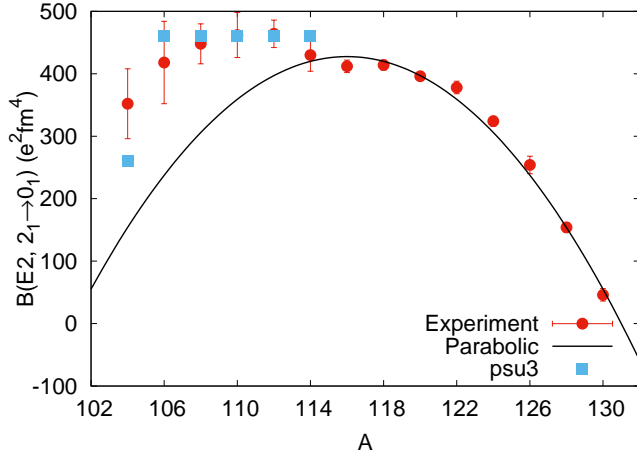


FIG. 1. The experimental  $B(E2 : 2_1^+ \rightarrow 0_1^+)$  for the Sn isotopes from compilations [1], compared with some arbitrary parabolic shape and pseudo-SU3 results to be explained here (squares).

seen in Fig. 1, a parabola accounts very well for their  $B(E2 : 2_1^+ \rightarrow 0_1^+)$  trend, except at  $^{112-114}\text{Sn}$ . That these early results (Jonsson *et al.* [2]) truly signaled a change of regime became evident through work on the unstable isomers, starting with the measurement in  $^{108}\text{Sn}$  by Banu *et al.* [3]. A flurry of activity followed [4–10], from which a new trend emerged in which the parabola, characteristic of a seniority scheme, gives way to a plateau, predicted by a pseudo-SU3 scheme (the squares). Here, I am going a bit fast, to follow the injunction of Montaigne: start by the last point (“Je veux qu’on comance par le dernier point” Essais II 10) [11, p. 296]. To slow down, I note that the idea to associate the plateau with pseudo-SU3, originated in a study of the cadmium isotopes, where quadrupole dominance is stronger and its consequences more clear-cut. Therefore, it is convenient to study the Cd and Sn families together. Section II provides the necessary tools.

## II. THEORETICAL FRAMEWORK

The basic idea is inspired by Elliott’s SU3 scheme [12, 13] and consists in building intrinsic determinantal states that maximize  $q_0$ , the expectation value of the quadrupole operator  $\hat{q}_0 = 2q_{20}$ , *i.e.*,  $q_0 = \langle 2q_{20} \rangle$  [14–16]. Fig. 2 implements the idea for  $^{104}\text{Cd}$  ( $Z = 48$ ,  $N = 56$ ). The single-shell contribution (S) of the  $g_{9/2} \equiv g$  proton orbit (Sg) is given by Eq.(1) (with changed sign for hole states) with  $m = 9/2$  being the first unfilled orbit for prolate deformation. For the neutron orbits, the pseudo-SU3 scheme [16–18] (P generically,  $Pr_p$  for specific cases) amounts to assimilating all the orbits of a major oscillator shell of principal quantum number  $p$ , except the largest (the  $r_p$  set) into orbits of

\* andres.zuker@in2p3.cnrs.fr

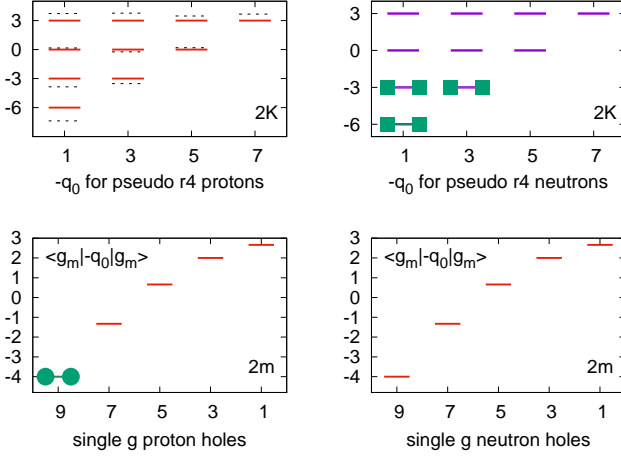


FIG. 2. The  $q_0$  diagrams for SP spaces adapted to the Cd and Sn isotopes. The (dimensionless)  $q_0 = \langle 2q_{20} \rangle$  values correspond to single particle and hole occupancies for the pseudo  $r_4$  ( $Pr_4$ ) and  $g$  cases respectively. The minus sign is an artifact to make occupancies start from the bottom. The figure illustrates the  $^{104}\text{Cd}$  configuration: circles for holes and squares for particles. The dashed lines are for  $\langle 2q_{20} \rangle$  from exact diagonalization.

the  $p - 1$  major shell. In our case the  $sdg$  shell has  $p = 4$ , and  $r_4$  is assimilated into a  $pf$  shell. As the  $\hat{q}_0$  operator is diagonal in the oscillator quanta representation, maximum  $\langle 2q_{20} \rangle$  is obtained by orderly filling states  $(n_z n_y n_x) = (300), (210), (201) \dots (012), (003)$ , with  $q_0 = \langle 2q_{20} \rangle = 2n_z - n_y - n_x = 6, 3, 3, 0, 0, \dots -3, -3$ , as in Fig. 2. Using  $q(n)$  for the cumulated  $q_0$  value (e.g. 24 for  $^{104}\text{Cd}$  in Fig. 2), the intrinsic quadrupole moment then follows as a sum of the single-shell (S) and pseudo-SU3 (P) contributions

$$q_0(S) = 2\langle r^2 C_{20} \rangle = \sum_m (p + 3/2) \frac{j(j+1) - 3m^2}{2j(j+1)} \quad (1)$$

$$q_0(P) = q(n), \quad Q_0(SP) = [(8e_\pi + q(n)e_\nu)b^2] \text{ efm}^2 \quad (2)$$

where I have introduced effective charges and recovered dimensions through  $Q = b^2 q$  with  $b^2 \approx 41.467/\hbar\omega \text{ fm}^2$  and  $\hbar\omega = 45A^{-1/3} - 25A^{-2/3}$ . To adapt Eq. (2) to Sn, simply drop the S part (*i.e.*, the  $8e_\pi$  term).

To qualify as a Bohr Mottelson rotor,  $Q_0(SP)$  must coincide with the intrinsic spectroscopic  $Q_{0s}$  and transition  $Q_{0t}$  quadrupole moments, defined through (as, e.g. in Ref. [16])

$$Q_{\text{spec}}(J) = \langle JJ | 3z^2 - r^2 | JJ \rangle$$

$$Q_{0s} = \frac{(J+1)(2J+3)}{3K^2 - J(J+1)} Q_{\text{spec}}(J), \quad K \neq 1 \quad (3)$$

$$B(E2, J \rightarrow J-2) = \frac{5}{16\pi} e^2 |\langle JK20 | J-2, K \rangle|^2 Q_{0t}^2 \quad (4)$$

$$K \neq 1 \quad B(E2 : 2^+ \rightarrow 0^+) = Q_0(SP)^2 / 50.3 \text{ e}^2 \text{ fm}^4 \quad (5)$$

TABLE I.  $B(E2 : 2_1^+ \rightarrow 0_1^+)$  estimates for  $^{98+n}\text{Cd}$  in  $\text{e}^2 \text{ fm}^4$  from Eq.(5). B20sp uses naive  $2q(n)_n$  cumulated pair occupancies diagonalization of  $\hat{q}_0$  in the  $pf$  shell *i.e.*, strict SU3, with  $(e_\nu, e_\pi) = (1.2, 1.5)$ . The B20SP numbers use (full)  $2q(n)_f$  from diagonalization of  $\hat{q}_0$  in the  $r_4$  space,  $(e_\nu, e_\pi) = (1.0, 1.4)$ . The  $b^2$  values range from  $4.83 \text{ fm}^2$  for  $A = 98$  to  $4.99 \text{ fm}^2$  for  $A = 110$ . Experimental values (B20e) for  $^{102-104}\text{Cd}$  are taken from [19] and [20], and from compilations [1] for  $^{106-110}\text{Cd}$ .

$A$	100	102	104	106	108	110
$n$	2	4	6	8	10	12
$2q(n)_n$	12	18	24	24	24	24
$2q(n)_f$	14.8	21.6	29.5	30.0	29.6	29.3
B20e	<560(4)	562(46)	779(80)	814(24)	838(28)	852(42)
B20sp	327	536	799	808	817	825
B20SP	317	511	795	824	817	813

To speak of deformed nuclei two conditions must be met:  $B(E2 : 4_1^+ \rightarrow 2_1^+)/B(E2 : 2_1^+ \rightarrow 0_1^+) = 1.43$  (the Alaga rule from Eq. (4)), and the “quadrupole quotient” rule,  $Q/q$  which follows from Eqs.(3) and (4) by equating  $Q_{0s} \approx Q_{0t}$  (for  $K = 0$ ):

$$50.27 B(E2 : 2^+ \rightarrow 0^+) / (3.5 Q_{\text{spec}})^2 = (Q/q)^2 \approx 1 \quad (6)$$

Full verification demands calculations but Eq. (5) can be checked directly by inspecting Fig. 2 as done in Table I, that will be analyzed once the shell-model results are in.

These results rely on diagonalizations in spaces defined by  $(g^{X-u} r_4^u)_\pi (g^{10-t} r_4^{n+t})_\nu$ ,  $X = 8$  for Cd and 10 for Sn. The proton ( $u$ ) and neutron ( $t$ ) excitations are restricted to have  $u + t \leq M$ . The calculations were done for  $utM = 000$  (the case in Fig. 2), 111, 101 and 202 using  $V_{\text{low-}k}$  variants [21] of the precision interaction N3LO [22] (denoted as I in what follows) with oscillator parameter  $\hbar\omega = 8.4 \text{ MeV}$  and cutoff  $\lambda = 2 \text{ fm}^{-1}$ . As a first step the monopole part of I is removed and replaced by single-particle energies for  $^{100}\text{Sn}$  from Ref. [23] referred to as GEMO for general monopole: a successful description of particle and hole spectra on magic nuclei from O to Pb, in particular consistent with the analysis of Ref. [24] for  $^{100}\text{Sn}$ . Specifically  $\epsilon_j = 0.0, 0.5, 0.8$  and  $1.6 \text{ MeV}$ . for  $j = 5/2, 7/2, 1/2$ , and  $3/2$ , respectively.)

The I interaction is then renormalized by increasing the  $\lambda\mu = 20$  quadrupole and  $JT = 01$  pairing components by  $q \times 10\%$  and  $p \times 10\%$ , respectively, and subject to an overall 1.1 scaling to account for renormalizations of other origins. The resulting interactions are called I.q.p. According to Ref. [25], the quadrupole renormalization (due to  $2\hbar\omega$  perturbative couplings) amounts to 30%, a theoretically sound result, empirically validated by the best phenomenological interactions in the  $sd$  and  $pf$  shells. By the same token the effective charges in  $0\hbar\omega$  spaces are estimated as  $(e_\nu, e_\pi) = (0.46, 1.31)$ , as

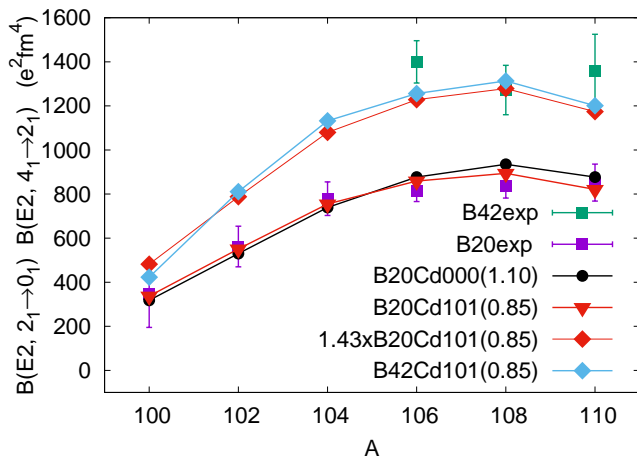


FIG. 3. Experimental and calculated  $B(E2)$  rates for the Cd isotopes, for different  $utM$  values.  $B(E2 : 2_1^+ \rightarrow 0_1^+)$  values from [19],[20], and [1].  $B(E2 : 4_1^+ \rightarrow 2_1^+)$  values from [28]. In parenthesis ( $e_\nu$ ),  $e_\pi = 1.40$  is fixed.

confirmed in Refs. [26, 27]. For the pairing component, perturbation theory is not a good guide, but comparison with the phenomenological interactions demands a 40% increase [15, 25]. It follows that I.3.4 and  $(e_\nu, e_\pi) = (0.46, 1.31)$  should be taken as standard for full  $0\hbar\omega$  spaces.

As I will be working in very truncated bases, which demand large effective charges, renormalizations should be implemented to account for polarization mechanisms that involve excitations to the  $g$  shell. Proton jumps will contribute to  $e_\nu$  and are expected to have greater impact than the corresponding neutron jumps, rapidly blocked by the  $(r_4^{n+t})_\nu$  particles. As a consequence, I set  $e_\pi = 1.4$ , a guess close to the standard value, and let  $e_\nu$  vary, thus becoming the only adjustable parameter in the calculations, a choice validated later in Sec. V.

### III. THE LIGHT Cd ISOTOPES

In Fig. 3 it is seen that  $utM = 000$  and  $101$  give the same results provided  $e_\nu$  is properly chosen. There is little difference between  $utM = 111$  and  $utM = 101$  because as soon as neutrons are added they block the corresponding jumps, as mentioned above.

The calculation exhibits near perfect agreement with the Alaga rule:  $(B(E2 : 4_1^+ \rightarrow 2_1^+)/B(E2 : 2_1^+ \rightarrow 0_1^+)) \approx 1.43B(E2 : 2_1^+ \rightarrow 0_1^+)$ . In the figure it is shown for  $utM = 101$  but it holds as well for  $000$  and  $111$ . The more stringent quadrupole quotient rule Eq. (6) yields an average  $Q/q = 0.96$  for  $^{106-110}\text{Cd}$ , corroborating the existence of a deformed region. As announced immediately after Eq. (6), Eq. (5) can be checked directly by inspecting Fig. 2, as done in Table I describing the “back of an envelope” SP estimates. Note that the naive form of P used so far (in  $q(n)_n$  and B20sp) is supplemented

by the more accurate  $q(n)_f$  and B20SP using fully diagonalized values of  $\langle 2q_{20} \rangle$ . The remarkable property of the  $r_4^n$  space that produces four identical  $q(n)_s$  values for  $n = 6 - 12$  has already been put to good use in Ref. [14] and Ref. [15, Fig. 38, TableVII]. In the present case, it is seen to do equally well.

It follows that the very simple estimates suggested by Fig. 2 are quantitatively reliable and can be associated with stable deformation in Cd. In Sn, the same estimates will remain reliable but they cannot be associated with stable deformation. A paradox examined in Sec. IV A.

My interest in the Cd isotopes was stimulated by the work of Schmidt and collaborators [29], an extension of Ref. [30], where the  $v3sb$  interaction (a renormalized version of the charge dependent Bonn potential [31]) was defined. The quadrupole coherence in these studies was clearly identified, but the  $B(E2 : 2_1^+ \rightarrow 0_1^+)$  plateau was missed. I obtained the interaction from Nadya Smirnova [32], and reproduced their results. If  $v3sb$  is made monopole free and the single particle spectrum replaced by the GEMO value for I.3.4, the  $B(E2 : 2_1^+ \rightarrow 0_1^+)$  pattern becomes identical to that of Fig. 3.

### IV. THE LIGHT Sn ISOTOPES

The basic tenet of this paper is that quadrupole dominance is responsible for the  $B(E2 : 2_1^+ \rightarrow 0_1^+)$  patterns in the light Cd and Sn isotopes, which means that they should exhibit a pseudo-SU3 symmetry. Hence, an intrinsic state should exist, implying the validity of the Alaga rule (Eq. (4)). The expectation is fulfilled in Cd (Fig. 3) but it fails in Sn, as seen in Fig. 4, where the  $B(E2 : 2_1^+ \rightarrow 0_1^+)$  rates are consistent with pseudo-SU3 validity, and are immune to details, while the  $B(E2 : 4_1^+ \rightarrow 2_1^+)$  rates are sensitive to the single-particle field and to the pairing strength. To test how the  $B(E2 : 4_1^+ \rightarrow 2_1^+)$  rates are influenced by the single particle field, the energy of the  $s_{1/2}$  orbit in  $^{101}\text{Sn}$  was displaced by 0.0, 0.4 and 0.8 MeV with respect to the present GEMO choice [23], called DZ (Duflo Zuker) in Ref. [24, Fig. 3.2.1] where an extrapolated value (EX) is given as reference. The position of the  $s_{1/2}$  orbit for DZ and EX differ by 800 keV. In the calculations reported in Fig. 4, I.3.4(0,0) and I.3.4(0.8) correspond to DZ and EX respectively. The  $B(E2 : 4_1^+ \rightarrow 2_1^+)$  differences are significant. Thanks to the recent  $^{108}\text{Sn}$   $B(E2 : 4_1^+ \rightarrow 2_1^+)$  measure of Siciliano *et al.* [33, Fig. 4b], the DZ choice is clearly favored.

#### A. The $B(E2 : 4_1^+ \rightarrow 2_1^+)/B(E2 : 2_1^+ \rightarrow 0_1^+)$ anomaly and the pairing-quadrupole interplay

The  $B(E2 : 4_1^+ \rightarrow 2_1^+)/B(E2 : 2_1^+ \rightarrow 0_1^+) < 1$  anomaly had been detected in  $^{114}\text{Xe}$  [34], in  $^{114}\text{Te}$  [35], and more recently in  $^{172}\text{Pt}$ , Ref. [36], where it is stressed

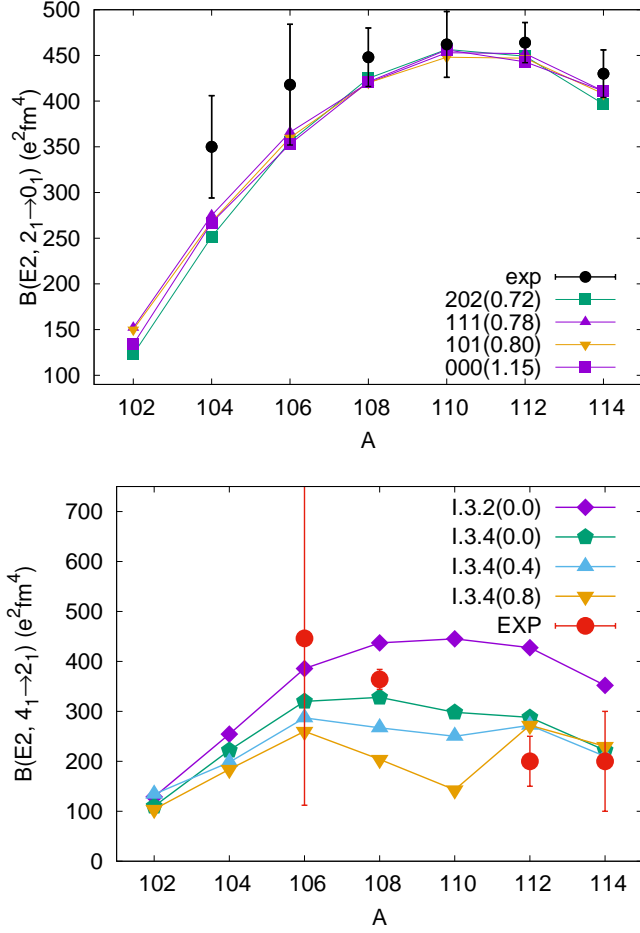


FIG. 4. Upper panel: Experimental [1] and calculated  $B(E2 : 2_1^+ \rightarrow 0_1^+)$  values for Sn isotopes with the I.3.4 interaction for different  $utM$  values. In parenthesis ( $e_\nu$ ),  $e_\pi = 1.40$  is fixed. Lower panel:  $B(E2 : 4_1^+ \rightarrow 2_1^+)$  data from Jonsson *et al.* [2] for  $^{112-114}\text{Sn}$ , and from Siciliano *et al.* [33] for  $^{106-108}\text{Sn}$ . I.3.2( $\delta$ ) and I.3.4( $\delta$ ) are  $utM = 202$  calculations with the  $s_{1/2}$  single-particle energy displaced by  $\delta = 0.0, 0.4$  and  $0.8$  MeV with respect to the GEMO value of  $0.8$  MeV.

that no theoretical explanation is available. Here, the sensitivity to the pairing strength provides a clue in Fig. 4, where its decrease in going from I.3.4 to I.3.2 produces a substantial increase of  $B(E2 : 4_1^+ \rightarrow 2_1^+)$ . The effect is seen most clearly in Ref. [33, Figs. 4a and 4b], where  $B(E2 : 2_1^+ \rightarrow 0_1^+)$  is seen to be totally immune to pairing, while  $B(E2 : 4_1^+ \rightarrow 2_1^+)$  is so sensitive that a sufficient decrease in strength could bring  $B(E2 : 4_1^+ \rightarrow 2_1^+)/B(E2 : 2_1^+ \rightarrow 0_1^+)$  close to the Alaga rule. It appears that pairing is eroding the deformed band. Only the lowest  $J = 0$  and  $2$  are spared, giving way to a pairing-quadrupole interplay, that will eventually end up in pairing dominance at  $N \approx 70$ . The transition region will be studied in Sec. VI.

## V. THE INTERACTION AND THE MODEL SPACES

Traditionally, the tin region was taken to be the prime example of pairing dominance, and calculations were based on seniority truncations which lead naturally to an overall parabolic trend, as shown schematically in Fig. 1.

The  $B(E2 : 2_1^+ \rightarrow 0_1^+)$  trend in the upper panel of Fig. 4, is already well reproduced by the neutron-only ( $utM = 000$ ) case. It will be shown that the monopole field is responsible for this welcome result. Though Bäck and coworkers [37, Fig. 3] already suggested that in such spaces the  $B(E2 : 2_1^+ \rightarrow 0_1^+)$  trend could be altered by changes in the single-particle behavior, their result was only indicative. The more complete calculations of Togashi *et al.* [38, Fig. 2] did better quanti-

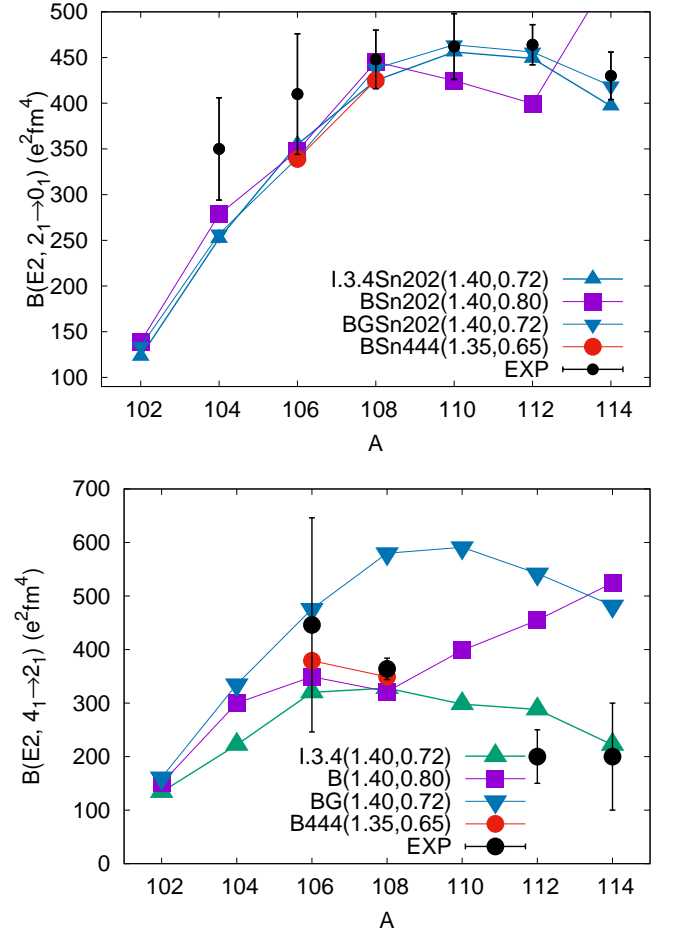


FIG. 5. Comparing  $B(E2 : 2_1^+ \rightarrow 0_1^+)$  for different  $utM$  values (upper panel) and  $B(E2 : 4_1^+ \rightarrow 2_1^+)$  (lower panel) calculations ( $utM = 202$ ) for B (the interaction used in Ref. [3], omitting the  $h_{11/2}$  orbit) and I.3.4 interactions in the Sn isotopes. BG is B made monopole free with the same GEMO single particle spectrum as I.3.4. In parenthesis ( $e_\pi, e_\nu$ ). Experimental data as in Fig. 4. See text.



tatively, but  $g$  proton excitations proved indispensable. (No  $B(E2 : 4_1^+ \rightarrow 2_1^+)$  estimates were given in this reference).

The difficulty in reproducing the  $B(E2 : 2_1^+ \rightarrow 0_1^+)$  enhancements for  $A < 114$  persists even when proton excitations are allowed in calculations [3, 6, 37] using the CDB (charge dependent Bonn) potential [31], renormalized following Ref. [39] (B in what follows). This raises two questions: why the I.3.4 interaction succeeds where others fail? and why the neutron-only description is not only viable, but the correct basic model space? They can be answered simultaneously and I start by explaining how severely truncated spaces may represent the exact results, by comparing the largest calculation available with smaller ones. In Ref. [33, Table I], results are given for  $^{106-108}\text{Sn}$  in  $utM = 444$  ( $m$ -dimensions  $10^{10}$ ) with the B interaction used in Banu *et al.* [3] (but omitting the  $h_{11/2}$  orbit). In Fig. 5 they are shown as B444 (circles) and compared with B202 (squares, the same interaction in our standard space). The agreement is very good for the two points in  $B(E2 : 2_1^+ \rightarrow 0_1^+)$  and  $B(E2 : 4_1^+ \rightarrow 2_1^+)$ . The result amounts to a splendid vindication of the shell model viewed as the possibility to describe in a small space the behavior of a large one. Although in general the reduction from large to small spaces demands renormalization of the operators involved, for our purpose, only the effective charges are affected, a non-trivial fact that invites further study.

Let me return now to the crucial role of the monopole field. In Fig. 5, the  $B(E2 : 2_1^+ \rightarrow 0_1^+)$  discrepancies between I.3.4 and B in the upper panel disappear when B is replaced by BG: the interaction made monopole free and supplemented by the GEMO single-particle field used in the I.q.p forces. For the  $B(E2 : 4_1^+ \rightarrow 2_1^+)$  pattern in the lower panel, the result is even more interesting: now BG is no longer close to I.3.4, but to I.3.0, which is not shown, but can be guessed by extrapolation in Fig. 4 (from I.3.4 to I.3.2) and from the type of multipole decomposition proposed in Ref. [25], revealing the same  $q \cdot q$  content in I.3.4 and BG, and a much weaker pairing for the latter; so weak in fact, that the BG results move closer to the Alaga rule.

It follows that for I.3.0, say, the  $Pr_4$  symmetry will hold, at least partially. As the pairing force is switched on, the  $J = 0_1, 2_1$  states are not affected, while  $J = 4_1$  is. This points to an unusual form of interplay between the two coupling schemes, pairing and quadrupole, traditionally associated with collectivity. In single fluid species, such as Sn, the seniority scheme can operate fully. It breaks down in the presence of two kinds of particles, which turns out to be the condition for quadrupole to operate successfully, as indicated by the Cd isotopes. What is unusual is the presence of quadrupole coherence in the light tins. It is shaky and challenged by pairing and it is known that at about  $A = 120$  the seniority scheme will prevail.

For the transition nuclei  $^{116-118}\text{Sn}$ , my original guess was that a mixing of spherical and weakly oblate states

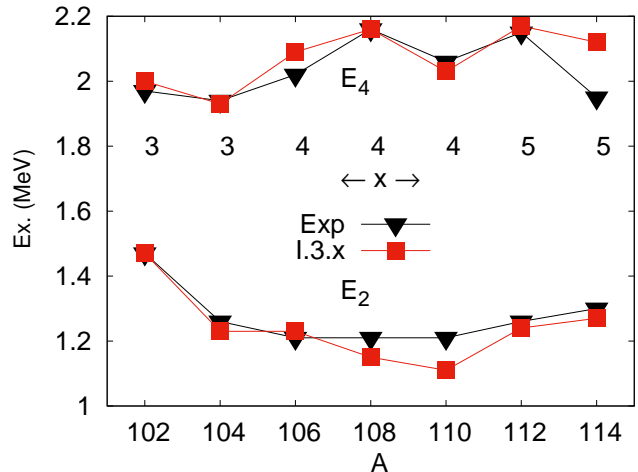


FIG. 6. Lowest  $E_2$  and  $E_4$  energies, calculated with I.3.x interactions.

TABLE II. Intrinsic adimensional  $q_0$  for prolate ( $q_0p$ ), and oblate ( $-q_0o$ ) states. Calculated spectroscopic quadrupole moments and g-factor  $Q_2, Q_4, g$  for I.3.4 ( $e_\nu, e_\pi$ ) = 0.72, 1.40;  $g_{s\nu} = -2.869$ ,  $g_{l\nu} = -0.070$  [40],  $g_{s\pi} = 4.189$ ,  $g_{l\pi} = 1.100$ . Experimental  $Q_2^*$  and  $g^*$  from Allmond *et al.* [41],  $g_{s\nu\pi}$  quenched by 0.75 with respect to bare values [15, Fig. 28].

N	$q_0p$	$-q_0o$	$Q_2$	$Q_4$	$Q_2^*$	$g^*$	$g$
52	12	6	-18	-24			-0.157
54	18	12	-21	-21			0.012
56	24	18	-16	-17			0.103
58	24	24	-5	-02			0.142
60	24	24	3	10			0.142
62	24	24	14	26	4(9)	0.150(43)	0.135
64	18	24	25	43	9(8)	0.138(63)	0.106

would take place. I also expected that neutron-only calculations, in which the monopole field would play a crucial role, would be likely to shed light on these matters. The guess was totally wrong, as explained in Sec. VI C. I mention this anecdote to stress that these two nuclei were the hardest to understand in the region.

Throughout this study, energy spectra have been ignored in favor of electromagnetic rates which are less sensitive to details, so I close by showing spectra for the lowest  $J = 2$  and 4 levels. In Fig. 6, some pairing state dependence has been allowed, but I.3.4 is seen to be the right overall choice.

## VI. Cd AND Sn AT $N \geq 64$

In Table II, the naive  $Pr_4$  adimensional intrinsic quadrupole moments for prolate ( $q_0p$ ) and oblate ( $q_0o$ ) are compared. The former are the same as  $q(n)_n$  in Table. I. The latter are obtained by filling the platforms

in reverse order (from the top). Up to  $N = 56$  prolate dominates. From  $N = 58$  to 62 there is oblate-prolate degeneracy. At  $N = 64$ , oblate dominates. In the absence of strong quadrupole dominance, these intrinsic values only indicate a trend in sign, respected by the calculated spectroscopic moments that opt for “oblate” shapes for  $A > 108$ . For  $^{112-114}\text{Sn}$ , the shell-model results are close for the quadrupole moments, or agree for the magnetic moments, with the measured values. Note: The magnetic moments are very sensitive to the anomalous  $g_{l\nu}$ .

By suggesting a very different behavior for the Sn and Cd and families at  $N=64$ , that will be examined in what follows, Table II illustrates the heuristic value of relying on pseudo-SU3, even when the symmetry does not hold in the strict sense.

So far the  $sdg$  space has proven sufficient, as the effects of the  $h_{11/2}$  orbit ( $h$  for short) remain perturbative. For Sn, it is known from classic  $(p, d)$  work [42], that the  $h$  occupancy, very small up to  $^{110}\text{Sn}$ , increases at  $^{112-114}\text{Sn}$ , as borne out by calculations that indicate the need of a boost of some 10% in  $B(E2 : 2_1^+ \rightarrow 0_1^+)$  [43] with respect to Fig. 4. Beyond  $N = 64$ , the explicit inclusion of the  $h$  orbit becomes imperative but the situation is different for the two families. In Sn, it is known that the traditional  $hr_4$  space will eventually prove sufficient when the seniority scheme takes over at  $N = 70$ . For  $^{116-118}\text{Sn}$ , at this stage, nothing can be said. For Cd, the calculations give systematically prolate values in line with Stone’s tables of quadrupole moments [44], but in  $^{112}\text{Cd}$  (excluded from both Table I and Fig. 3) they yield severe underestimates whose correction necessitates the introduction of a quasi-SU3 mechanism (referred generically as Q in what follows, and  $Qhfp$  for the case I introduced next). It is illustrated in Fig. 7, where it is seen that at  $N = 64$ , promoting an extra particle to the  $q_0 = -3$  platform reduces prolate coherence in Cd, while filling the seven upper platforms makes it possible for  $^{114}\text{Sn}$  to stay oblate. To obtain realistic estimates demands calculating the quadrupole moment in the presence of a central field. An economic way of doing so is through Nilsson-SU3 self-consistency [16], which is explained next.

#### A. Nilsson-SU3 self-consistency in a SPQ context

Let us start by remembering that  $q_0 = \langle 2q_{20} \rangle$ , decompose it, together with the corresponding operator  $\hat{q}_0$ , into the S, P and Q contributions, and introduce the normalized variant  $q_{0N}$ . Then examining Ref.[16, Eq.(19)]

$$\hat{q}_{0N} = \frac{\hat{q}_{\pi S}}{\mathcal{N}_4} + \frac{\hat{q}_{\nu P}}{\mathcal{N}_4} + \frac{\hat{q}_{\nu Q}}{\mathcal{N}_5}, q_{0N} = \frac{q_{\pi S}}{\mathcal{N}_4} + \frac{q_{\nu P}}{\mathcal{N}_4} + \frac{q_{\nu Q}}{\mathcal{N}_5} \quad (7)$$

$$H = H_{sp} - \frac{\hbar\omega\delta}{3}\hat{q}_0 \equiv H_{sp} - \beta\hbar\omega\kappa\hat{q}_{0N}q_{0N} \quad (8)$$

$$\mathcal{N}^2 = \sum (2q_{20rs})^2 = \sum_{k=0}^p (k+1)(2p-3k)^2. \quad (9)$$

( $p$  is the principal quantum number). Eq. (8) compares the classic Nilsson problem to the left and the self-consistent version to the right, which demands the solution of a linearized  $\kappa\hbar\omega\hat{q}_0 \cdot \hat{q}_0/\mathcal{N}^2$  problem, taken to approximate Elliott’s quadrupole force, in its correct realistic normalized form, which involves the inclusion of the norm in Eq. (9), as demonstrated in Ref. [25]. The coupling constant,  $\kappa = 3$ , is the same as in interactions I.3.x, while  $H_{sp}$  is taken from GEMO [23]. The quantity I am after,  $q_0$ , is calculated while in the Nilsson case it is simply the parameter  $\delta$ .

The self-consistent solution of the problem is obtained by demanding that that input and output  $q_{0N}$  coincide. Calculations are done for each space separately. To ensure that the couplings involve the full  $q_0$ , a parameter  $\beta_X$  is introduced:

$$\frac{\hat{q}_{\nu P}}{\mathcal{N}_4^2}(q_{\pi S} + q_{\nu P}) \longrightarrow \beta_P \frac{\hat{q}_{\nu P}}{\mathcal{N}_4^2} q_{\nu P} \quad (10)$$

$$\frac{\hat{q}_{\nu Q}}{\mathcal{N}_5^2}(q_{\nu Q} + (q_{\pi S} + q_{\nu P})\frac{\mathcal{N}_5}{\mathcal{N}_4}) \longrightarrow \beta_Q \frac{\hat{q}_{\nu Q}}{\mathcal{N}_5^2} q_{\nu Q} \quad (11)$$

At each iteration a full spectrum of Nilsson-like energies  $\varepsilon(2k, i)$  is generated, from which quadrupole contributions  $q_0(2k, i)$  are extracted by subtracting the  $H_{sp}$  part. The full  $q_0$  is the sum of all such contributions for a given  $A$ . In the case of  $^{110}\text{Cd}$  in Fig. 7, it involves the six filled P-platforms. According to Eq. (10), this is the quantity to be extracted self-consistently. However, it turns out that the results are little changed if it is replaced by the single lowest contribution. In other words, in  $^{110}\text{Cd}$   $\beta_P$  may range from 1.3 for the full  $q_0 = q_{\nu P}$  to 2.8 for  $q_0(1, 1)$ , for nearly identical final results  $q_0 = q_{\nu P} = 13.0(3)$ , or 26.0(6) (for pair occupancy) to be compared with 24 and 29.3, the values in Table I in the absence of monopole field. Hence: the elementary SP arguments in Table I, the diagonalizations in Fig. 3, and the present self-consistent results nearly coincide. This is a pleasant result.

At  $N = 64$  and beyond, Eq. (11) applies. Since  $\mathcal{N}^2 = 210$  and 420 for  $p = 4$  and 5 respectively,  $(q_{\pi S} + q_{\nu P})\mathcal{N}_5/\mathcal{N}_4 = (4 + 13)\sqrt{2} \approx 24$ . The self-consistent calculations in Table III are done using  $q_0 = q_0(1, 1) + q_0(3, 1)$  input-output values and  $\beta_Q = 4$ , consistent with  $q_{\nu Q} = 8.06$  in the table, as  $(24+8)/8=4$ .

In results so far, involving P and Q spaces (Refs. [14] for the rare earth, [16] for  $N = Z$  nuclei and for  $N < 64$  in the present study), the influence of  $H_{sp}$  is relatively minor, and  $B(E2 : 2_1^+ \rightarrow 0_1^+)$  rates remain close to their theoretical maxima represented by the  $q_0$  diagrams. For the Q case, described in Table III,  $H_{sp}$  plays a major role, and I have chosen to present together the results for the strict  $Qhfp_f$  and self-consistent cases ( $Q_f$  and SC in what follows).

Under  $\phi_h^2$ , I have listed the squared amplitude of the  $h = h_{11/2}$  components of the wave functions. They are on the average of about 56% for  $Q_f$  and 98% for SC, leading to different filling patterns.

TABLE III. Quantities entering schematic and self-consistent calculations for  $^{112-122}\text{Cd}$  ( $N = 64 - 74$ ). Single particle spectrum at  $^{115}\text{Sn}$  from GEMO [23].  $\epsilon(h_{11/2}) = 0$ ,  $\epsilon(f_{7/2}) = 3.6$ ,  $\epsilon(p_{3/2}) = 5.4$  MeV. See text for detailed explanations.

Qhfp <sub>f</sub> (Q <sub>f</sub> )						
$2ki$	11	31	51	12	71	32
$\phi_h^2$	0.21	0.43	0.69	0.61	0.89	0.51
$q_0(2k, i)$	8.55	6.06	3.28	2.96	0.50	0.50
$N$	64	66	68	70	72	74
$q_{\nu Q}(N)$	8.55	14.61	17.89	20.85	21.35	21.65
$e_{\nu}(N)$	0.75	0.60	0.55	0.50	0.50	0.50
$B(E2, A)$	1016	1049	1095	1095	1130	1165
Self consistent (SC)						
$2ki$	11	31	51	71	91	111
$\phi_h^2$	0.97	0.98	0.99	0.99	1.00	1.00
$\epsilon(2k, i)$	-0.72	-0.59	-0.35	-0.01	0.43	0.94
$q_0(2k, i)$	4.44	3.62	2.13	0.13	-2.27	-5.00
$A$	112	114	116	118	120	122
$q_{\nu Q}(A)$	4.44	8.06	10.19	10.32	8.05	3.05
$e_{\nu}(A)$	0.95	0.83	0.78	0.78	0.75	0.75
$B(E2, A)$	984	1078	1148	1169	934	655

The filling patterns ( $2ki$ ) as a function of  $A$  are those of Fig. 7 for  $Q_f$ , but are dictated by the energies  $\epsilon(2k, i)$  in MeV for SC, in which case the  $q_0(2k, i)$  values are not necessarily the largest possible.

In particular,  $q_0(1, 2) \approx 5$  is the largest, but it has a huge energy  $\epsilon(1, 2) = 2.82$  MeV, and  $\phi_h^2 \approx 0$ . The (12) orbit will play two roles in what follows: as a purveyor of intruders and as signaling a transition between two deformed regimes.

The  $B(E2, A) = B(E2 : 2_1^+ \rightarrow 0_1^+)$  rates, with  $e_{\nu}(A)$  from Table III, are calculated through

$$B(E2 : 2_1 \rightarrow 0_1) = [2(q_{\pi S}e_{\pi} + (q_{\nu P} + q_{\nu Q})e_{\nu})b^2]^2/50.3, \quad (12)$$

where  $q_{\pi S} = 4$ ,  $e_{\pi} = 1.4$ , and  $q_{\nu P} = 13$ , as calculated earlier. To account for rearrangements in the P space when Q pairs are added  $q_{\nu P} = 14$  would also do, without affecting the satisfactory agreement with data in Fig. 8. To explain the  $e_{\nu}(A)$  choices, I start recalling that they are associated with  $2\hbar\omega$  and  $0\hbar\omega$  contributions, described in the paragraphs preceeding Sec. III. Up to  $N = 64$ , the  $0\hbar\omega$  part is mediated by quadrupole jumps coupling  $r_4$  neutrons to proton particle-hole excitations from the  $g$  orbit. For  $N \geq 64$  the couplings are increasingly mediated by  $hfp$ , *i.e.*,  $p = 5$  neutrons, leading to a suppression of quadrupole strength, due to the  $\mathcal{N}_5/\mathcal{N}_4$  norm effect that has been encountered earlier. As a consequence  $e_{\nu}$  is expected to decrease gradually as the  $r_4$  orbits fill and reduce their contribution. The alternative is a constant, plausible for  $N > 64$  but not at  $N = 64$ , which definitely demands a larger  $e_{\nu}$ . Once the gradual decrease is accepted, the choice in Table III is quite constrained

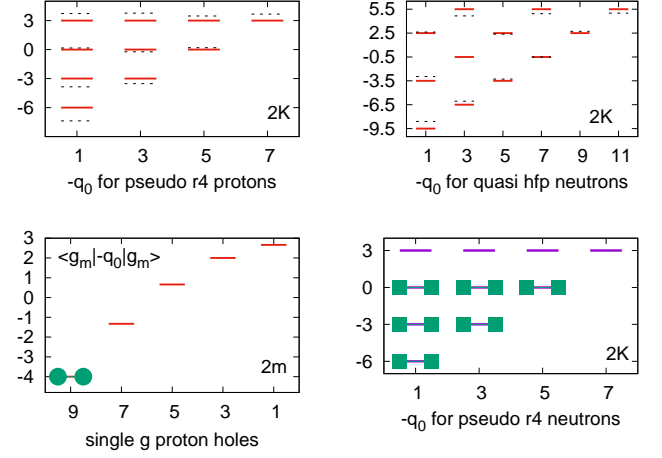


FIG. 7. The  $^{110}\text{Cd}$  intrinsic state in the SPQ space. The schematic pseudo-SU3 platforms  $Pr_{4s}$  are obtained by diagonalizing the  $\hat{q}_0$  operator in the  $p = 3$  space (full lines), while dashed lines correspond to the full  $\hat{q}_0$  in the  $r_4$  space ( $Pr_{4f}$ ). The quasi-SU3 ( $Qhfp_s$ )  $q_0$  platforms (full lines) are obtained by diagonalizing the quasi-quadrupole operator in the  $hfp$  space *i.e.*, the degenerate  $\Delta J = 2$  sequence in  $pfh$  shell:  $h_{11/2}$ ,  $f_{7/2}$ ,  $p_{3/2}$ . Dashed lines ( $Qhfp_f$ ) are for the full quadrupole operator. The quasi-quadrupole operator is obtained by using the  $l \cdot s$  form of the  $\hat{q}$  matrix elements and then replacing  $l$  by  $j = l + 1/2$  [16, Section IIIC].

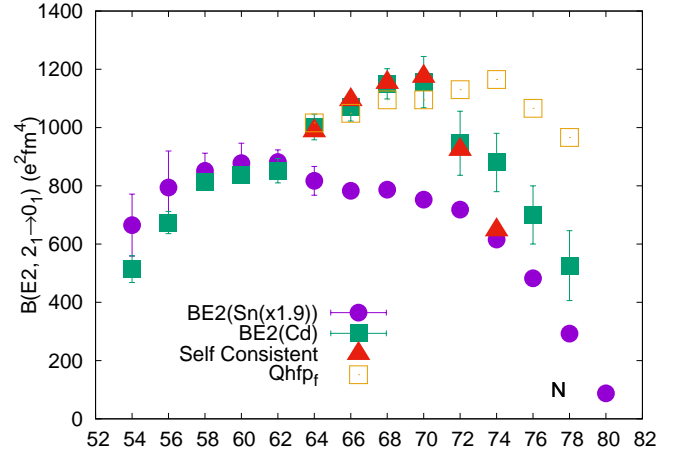


FIG. 8. The observed  $B(E2 : 2_1^+ \rightarrow 0_1^+)$  values for Cd and Sn, and the schematic and self-consistent estimates for Cd at  $N = 64$  and beyond. Note that the Sn values are boosted by a 1.9 factor.

and the good agreement in Fig. 8 follows naturally. The table and Eq.(12) contain all that is needed to explore alternatives, but they will hardly change the quality of the agreement.

Independently of details, there are two indications that the calculations are on track: the drop at  $^{120}\text{Cd}$ ,  $N = 72$ ,

and the strong underestimate at  $^{122}\text{Cd}$  which signals the transition to oblate states, suggested by Stone's tables of quadrupole moments [44]. The point is delicate because the signs depend on the  $K$  values (Eq. (3)). The hint comes from the  $h_{11/2}$  values, systematically negative up to  $^{119}\text{Cd}$ , and positive beyond.

The two indications are probably correlated and invite further study.

## B. Cd prospects: vibration, intruders, coexistence

Arguably, the most striking feature of the self-consistent calculation is the overwhelming dominance of the  $h = h_{11/2}$  orbit, which makes it impossible to speak of a quasi-SU3 symmetry, though one works in a Q space. The results of calculations in the full  $p = 5$  space, using  $H_{sp}$  from GEMO [23], are nearly identical to those in the Q space, which is vindicated as the correct choice. The transition between the  $Q_f$  and SC regimes can be followed through variations of the  $H_{sp}$  splittings. At  $\epsilon(h_{11/2}) = 0$ ,  $\epsilon(f_{7/2}) = 2.0$ ,  $\epsilon(p_{3/2}) = 3.0$  MeV,  $\phi_h^2 = 0.89$  and the SC filling pattern remains unchanged, but with a further reduction:  $\epsilon(h_{11/2}) = 0$ ,  $\epsilon(f_{7/2}) = 1.0$ ,  $\epsilon(p_{3/2}) = 2.0$  MeV,  $\phi_h^2 = 0.66$  the patterns change to  $Q_f$ , as the  $2ki = 12$  orbit fills at  $N = 72$ : there is a change in regime from SC to  $Q_f$ . As to what is SC in Table III, an answer is suggested in the tables [28]: the nuclei must be vibrational since  $B(E2 : 4_1^+ \rightarrow 2_1^+)/B(E2 : 2_1^+ \rightarrow 0_1^+) \approx 2$ . The problem is that vibrational nuclei are not supposed to be deformed, as pointed out by Tamura and Udagawa [45] after the observation of a large static quadrupole moment in  $^{114}\text{Cd}$ . After half a century, the question remains open [46, 47], though attempts have been made to modify the vibrational model so as to make it viable [48]. As of now, I adopt a Gordian-knot solution and call such states q-vibrational. The precise definition will be given in Sec. VID.

In introducing the SPQ spaces, I expected  $^{112-116}\text{Cd}$  to behave as weakly deformed states in analogy to their lighter counterparts, but something different is happening, as made clear in the calculations. In [46, Fig. 5] the contrast is clear:  $^{110}\text{Cd}$  follows the Alaga rule, while  $B(E2 : 4_1^+ \rightarrow 2_1^+)/B(E2 : 2_1^+ \rightarrow 0_1^+) = 2$  for  $^{112-116}\text{Cd}$ .

Recent beyond mean field (BMF) calculations in  $^{110,112}\text{Cd}$  [49] are fairly successful at describing the numerous coexisting states. Referring to Fig. 7, it is easy to visualize how such states could be produced by promoting  $q_0 = 0$  P pairs to the  $Q_f$  space. Thus, promoting the  $2ki = 12$  pair with  $q_0(1, 2) \approx 5$  on top of  $^{112-114}\text{Cd}$  ground states leads to  $q_{\nu Q} \approx 9$  and 13 respectively, using  $e_{\nu}$  from Table III, and then  $B(E2 : 2_3^+ \rightarrow 0_2^+) = 47$  and 48 W.u., respectively, against the observed 51(12) and 65(9) W.u. The case of  $^{110}\text{Cd}$  does not demand calculations but a check: its  $B(E2 : 2_3^+ \rightarrow 0_2^+) = 29(5)$  W.u. should be the same as  $B(E2 : 2_1^+ \rightarrow 0_1^+) = 30.3(2)$  in  $^{112}\text{Cd}$ . They are. The experimental values are from [1, 46, 49].

The calculations and estimates so far, are useful in describing  $B(E2 : 2_1^+ \rightarrow 0_1^+)$  trends but the determinant test rests with the  $B(E2 : 4_1^+ \rightarrow 2_1^+)/B(E2 : 2_1^+ \rightarrow 0_1^+)$  ratios. In the case of the light Cd isotopes, it was met by shell-model calculations, but the irruption of the Q space puts them beyond reach for  $N \geq 64$ . The BMF spectra are of little help, as they yield ratios too large compared to the Alaga rule in  $^{110}\text{Cd}$  (1.66), and below the vibrational limit in  $^{112}\text{Cd}$  (1.71) [49]. So, I propose to try something different.

### 1. Band Coupling

The idea is to prediagonalize the Hamiltonian in the SP and Q subspaces and couple the resulting bands to form a basis  $J_{SP} \otimes J_Q$ .

In all probability, something similar has been proposed in the past, but I know of no successful implementation, probably because of the difficulty of defining the correct interaction to be used in the individual spaces, as can be understood by concentrating on the quadrupole force. The naive view is that, if  $k\hat{q} \cdot \hat{q}$  is used in the full space, then the same should be used in each of the subspaces. What has been learned is that the correct choice is to change  $k \rightarrow \beta k$ . Though no calculations in the coupled basis will be attempted here, some runs were made in the Q or SQ spaces,  $hfp_{\nu}^{2-10}$  or  $(h_{\pi}^{10})(hfp_{\nu}^{2-10})$  (replacing  $g_{\pi}^8$  by  $h_{\pi}^{10}$ , for simplicity) with a large quadrupole force and with the realistic I interaction with the same quadrupole strength. The results with both interactions very much coincide with those of the SC calculations for  $B(E2 : 2_1^+ \rightarrow 0_1^+)$  but nothing close enough to  $B(E2 : 4_1^+ \rightarrow 2_1^+)/B(E2 : 2_1^+ \rightarrow 0_1^+) = 2$  emerged. It is to be hoped that it will happen once the coupling to the SP space is implemented. Still, the rudimentary calculations confirmed that the quadrupole force determines the coupling scheme, and that, even with very large  $H_{sp}$  splittings, and overwhelming  $h_{11/2}$  dominance, prolate solutions prevailed, even for two particles. I propose to call such states  $h^2$ -prolate. They will prove important in what follows.

## C. Sn prospects in A=116 and 118.

Following Montaigne again, I start with a spoiler:  $^{116-118}\text{Sn}$  are most probably q-vibrational nuclei. In spite of the spoiler, the story is of interest. At  $N = 64$ , the interaction favors oblate in Table II (consistent with data in Allmond *et al.* [41]), and the calculations do well, (Fig. 3). For Cd, there is a change in regime marked by a jump in Fig. 8. For Sn, there is a smooth inflection point, inviting the idea of a smooth transition. The natural assumption of an oblate  $^{116}\text{Sn}$ , obtained by adding an  $h_{11/2}^2$  pair does not work for two reasons. The first is that the  $B(E2 : 2_1^+ \rightarrow 0_1^+)$  of about 700-800  $e^2\text{fm}^4$  or 20-24 W.u. (adapting Eq. (12), eliminating protons and



replacing  $q_{\nu Q}$  by  $q_{\nu h} = -5$ ), is double the observed value. The second is that  $^{116}\text{Sn}$  is prolate [44]. The way out is to use the prolate solution in Table II, *i.e.*,  $q_{\nu P} = 18$  rather than -24, and  $h^2$ -prolate *i.e.*,  $q_{\nu Q} = 4.44$  from Table III in Eq. (12) to obtain 12.1 W.u. for  $e_\nu = 1.05$ , against the observed 12.4(4) W.u.

All this may seem far fetched, but the corroborating evidence is strong: as  $B(E2 : 4_1^+ \rightarrow 2_1^+) = 38(24)$  W.u., the  $B(E2 : 4_1^+ \rightarrow 2_1^+)/B(E2 : 2_1^+ \rightarrow 0_1^+)$  quotient becomes vibrational-compatible. For  $^{118}\text{Sn}$ , the situation is similar.

#### D. q-vibrations

The total coincidence between Cd and Sn  $B(E2 : 2_1^+ \rightarrow 0_1^+)$  patterns in Fig. 8 at  $N < 64$  was challenged by the  $B(E2 : 4_1^+ \rightarrow 2_1^+)/B(E2 : 2_1^+ \rightarrow 0_1^+)$  quotients, which ironically establish their similarity at  $N \geq 64$  where they diverge abruptly. I have used the term q-vibrational for the latter region. It applies to states that fulfill two conditions: a)  $B(E2 : 4_1^+ \rightarrow 2_1^+)/B(E2 : 2_1^+ \rightarrow 0_1^+)$  and  $E_4/E_2 \approx 2$ , and b) sizable quadrupole moment of non-rotational origin, as calculated in the previous Secs. VIB and VIC. Condition b ensures a situation similar to that encountered at the beginning of this study: the encouraging SP suggestions for  $B(E2 : 2_1^+ \rightarrow 0_1^+)$  were validated by further shell-model work, still missing here, but expected to work equally well.

It could be objected that postulating q-vibrations is a bold step that relies too heavily on data. Certainly, but to explain why  $B(E2 : 4_1^+ \rightarrow 2_1^+)/B(E2 : 2_1^+ \rightarrow 0_1^+)$  is smaller than one in  $^{114}\text{Sn}$  and about two in  $^{116}\text{Sn}$  one has to be a bit bold. And remember that the speculations rest on credible  $B(E2 : 2_1^+ \rightarrow 0_1^+)$  estimates.

### VII. CONCLUSIONS

For a summary of what has been achieved in this paper, I refer to the “Results” item of the abstract, and concentrate here on the basic ingredients at the origin of the good results: the interaction and specifically, the monopole Hamiltonian, and the SPQ interpretive framework.

**The Interaction:** The shell-model Hamiltonian can be separated into a monopole part,  $H_m$ , that contains all quadratic terms in number operators, and a multipole part,  $H_M$ , that contains all the rest, and is

dominated by pairing and quadrupole components that demand a renormalization for use in restricted spaces. While  $H_M$  depends very little on the realistic potential chosen [15, II D], and does well spectroscopically,  $H_m$ , responsible for saturation properties and single-particle behavior, usually necessitates *ad hoc* fits, adapted to the problem at hand. In this work, I have relied on the general monopole Hamiltonian GEMO [23], that reproduces, within a root mean square error of 200 keV, the particle and hole spectra on double-magic nuclei.

**The monopole interaction:** A key step in the implementation is to eliminate the monopole part  $H_m$  and use the GEMO single-particle field, eventually modulated by the total number of active particles; not necessary for  $N < 64$  but essential beyond, when the  $h_{11/2}$  orbit comes in. The GEMO choice has been found to ensure correct  $B(E2 : 2_1^+ \rightarrow 0_1^+)$  and  $B(E2 : 4_1^+ \rightarrow 2_1^+)$  patterns in Figs. 3, 4 and 5, and has lead to a prediction for the position of the  $s_{1/2}$  orbit in  $^{101}\text{Sn}$ .

Conceptually, GEMO has made it possible to establish the neutron-only description in the tin isotopes as the natural starting model space.

**The SPQ interpretive framework and self consistency:**

In doing calculations, the aim is not only to reproduce data, but also to understand underlying mechanisms. The SPQ representations, in addition to their predictive power, have served this purpose well. They are also the backbone of Nilsson-SU3 selfconsistent estimates that supplement existing calculations and open the way to future ones, as in Fig. 8.

In this paper, calculations have alternated between full rigor, heuristics and semi-quantitative estimates, regions have moved from well-developed deformed, to pairing-quadrupole coexistence, to the newly postulated q-vibrational states. Cadmium and tin come and go. “The world is but a perennial swing” (Le monde n’est qu’une branloire perenne. Essais III 2 [11, p. 582]).

### ACKNOWLEDGMENTS

Alfredo Poves and Frédéric Nowacki took an active interest in the paper and made important suggestions. The collaboration with Marco Siciliano, Alain Goasduff and José Javier Valiente Dobón is gratefully acknowledged.

---

[1] B. Pritychenko, M. Birch, B. Singh, and M. Horoi, Tables of  $e2$  transition probabilities from the first  $2^+$  states in even-even nuclei, *At. Data Nucl. Data Tables* **107**, 1 (2016), erratum *ibid.* **114**, 371 (2017).

[2] N.-G. Jonsson, A. Bäcklin, J. Kantele, R. Julin, M. Luontama, and A. Passoja, Collective states in even Sn nuclei, *Nucl. Phys. A* **371**, 333 (1981).

[3] A. Banu, J. Gerl, C. Fahlander, M. Górska, H. Grawe,

- T. R. Saito, H.-J. Wollersheim, E. Caurier, T. Engeland, A. Gniady, M. Hjorth-Jensen, and F. Nowacki,  $^{108}\text{Sn}$  studied with intermediate-energy Coulomb excitation, *Phys. Rev. C* **72**, 061305(R) (2005).
- [4] C. Vaman *et al.*,  $Z = 50$  shell gap near  $^{100}\text{Sn}$  from intermediate-energy Coulomb excitations in even-mass  $^{106-112}\text{Sn}$  isotopes, *Phys. Rev. Lett.* **99**, 162501 (2007).
- [5] A. Ekström, J. Cederkäll, C. Fahlander, A. Hurst, M. Hjorth-Jensen, *et al.*, Sub-barrier Coulomb excitation of  $^{110}\text{Sn}$  and its implications for the  $^{100}\text{Sn}$  shell closure, *Phys. Rev. Lett.* **98**, 172501 (2007).
- [6] A. Ekström, J. Cederkäll, C. Fahlander, M. Hjorth-Jensen, *et al.*,  $0_{gs}^+ \rightarrow 2_1^+$  transition strengths in  $^{106}\text{Sn}$  and  $^{108}\text{Sn}$ , *Phys. Rev. Lett.* **101**, 012502 (2008).
- [7] R. Kumar, P. Doornenbal, A. Jhingan, R. K. Bhowmik, S. Muralithar, *et al.*, Enhanced  $0_{g.s.}^+ \rightarrow 2_1^+$   $E2$  transition strength in  $^{112}\text{Sn}$ , *Physical Review C* **81**, 024306 (2010).
- [8] V. M. Bader, A. Gade, D. Weisshaar, *et al.*, Quadrupole collectivity in neutron-deficient Sn nuclei:  $^{104}\text{Sn}$  and the role of proton excitations, *Phys. Rev. C* **88**, 051301(R) (2013).
- [9] P. Doornenbal, S. Takeuchi, N. Aoi, M. Matsushita, A. Obertelli, D. Steppenbeck, H. Wang, *et al.*, Intermediate-energy Coulomb excitation of  $^{104}\text{Sn}$ : Moderate  $E2$  strength decrease approaching  $^{100}\text{Sn}$ , *Phys. Rev. C* **90**, 061302(R) (2014).
- [10] R. Kumar, M. Saxena, P. Doornenbal, A. Jhingan, *et al.*, No evidence of reduced collectivity in Coulomb-excited Sn isotopes, *Phys. Rev. C* **96**, 054318 (2017).
- [11] M.-L. Demonet, A. Legros, M. Duboc, L. Bertrand, and A. Lavrentiev, *Michel de Montaigne, Essais, 1588 (Exemplaire de Bordeaux), édition numérique générique (XML-TEI/ PDF)*, edited by M.-L. Demonet (2016).
- [12] J. P. Elliott, Collective motion in the nuclear shell model. I. Classification schemes for states of mixed configurations, *Proc. R. Soc. London* **245**, 128 (1958).
- [13] J. P. Elliott, Collective motion in the nuclear shell model II. The introduction of intrinsic wave-functions, *Proc. R. Soc. London* **245**, 562 (1958).
- [14] A. P. Zuker, J. Retamosa, A. Poves, and E. Caurier, Spherical shell model description of rotational motion, *Phys. Rev. C* **52**, R1741 (1995).
- [15] E. Caurier, G. Martínez-Pinedo, F. Nowacki, A. Poves, and A. P. Zuker, The shell model as a unified view of nuclear structure, *Rev. Mod. Phys.* **77**, 427 (2005).
- [16] A. P. Zuker, A. Poves, F. Nowacki, and S. M. Lenzi, Nilsson-SU3 self-consistency in heavy  $N = Z$  nuclei, *Phys. Rev. C* **92**, 024320 (2015).
- [17] A. Arima, M. Harvey, and K. Shimizu, Pseudo  $LS$  coupling and pseudo  $SU_3$  coupling schemes, *Phys. Lett. B* **30**, 517 (1969).
- [18] K. T. Hecht and A. Adler, Generalized seniority for favored  $J \neq 0$  pairs in mixed configurations, *Nucl. Phys. A* **137**, 129 (1969).
- [19] A. Ekström, J. Cederkäll, D. D. DiJulio, C. Fahlander, and M. Hjorth-Jensen, Electric quadrupole moments of the  $2_1^+$  states in  $^{100,102,104}\text{Cd}$ , *Phys. Rev. C* **80**, 054302 (2009).
- [20] N. Boelaert, A. Dewald, C. Fransen, J. Jolie, A. Linnemann, B. Melon, O. Möller, N. Smirnova, and K. Heyde, Low-spin electromagnetic transition probabilities in  $^{102,104}\text{Cd}$ , *Phys. Rev. C* **75**, 054311 (2007), erratum *ibid.* **77**, 019901 (2008).
- [21] S. Bogner, T. T. S. Kuo, and A. Schwenk, Model-independent low momentum nucleon interaction from phase shift equivalence, *Phys. Rep.* **386**, 1 (2003).
- [22] D. R. Entem and R. Machleidt, Accurate nucleon-nucleon potential based upon chiral perturbation theory, *Phys. Lett. B* **524**, 93 (2002).
- [23] J. Duflo and A. P. Zuker, The nuclear monopole Hamiltonian, *Phys. Rev. C* **59**, R2347 (1999), program gemosp9.f in the archive Duflo-Zuker-program.zip from <https://www-nds.iaea.org/amdc/>.
- [24] T. Faestermann, M. Górska, and H. Grawe, The structure of  $^{100}\text{Sn}$  and neighbouring nuclei, *Prog. Part. Nucl. Phys.* **69**, 85 (2013).
- [25] M. Dufour and A. P. Zuker, Realistic collective nuclear Hamiltonian, *Phys. Rev. C* **54**, 1641 (1996).
- [26] H. L. Crawford, R. M. Clark, P. Fallon, and A. O. Macchiavelli, Quadrupole collectivity in neutron-rich Fe and Cr isotopes, *Phys. Rev. Lett.* **110**, 242701.
- [27] A. Blazhev, M. Górska, H. Grawe, J. Nyberg, M. Palacz, E. Caurier, O. Dorvaux, A. Gadea, and F. Nowacki, Observation of a core-excited  $E4$  isomer in  $^{98}\text{Cd}$ , *Phys. Rev. C* **69**, 064304 (2004).
- [28] <https://www.nndc.bnl.gov/nudat2>.
- [29] T. Schmidt, K. L. G. Heyde, A. Blahzev, and J. Jolie, Shell-model-based deformation analysis of light cadmium isotopes, *Phys. Rev. C* **96**, 014302 (2017).
- [30] N. Boelaert, N. Smirnova, K. Heyde, and J. Jolie, Shell model description of the low-lying states of light cadmium isotopes, *Phys. Rev. C* **75**, 014316 (2007).
- [31] R. Machleidt, F. Sammarruca, and Y. Song, Nonlocal nature of the nuclear force and its impact on nuclear structure, *Phys. Rev. C* **53**, R1483 (1996).
- [32] N. Smirnova, The v3sb interaction, private communication (2017).
- [33] M. Siciliano, J. J. Valiente-Dobón, A. Goasduff, F. Nowacki, A. P. Zuker, *et al.*, Pairing-quadrupole interplay in the neutron-deficient tin nuclei: First lifetime measurements of low-lying states in  $^{106,108}\text{Sn}$ , *Phys. Lett. B* **806**, 135474 (2020).
- [34] G. de Angelis, A. Gadea, E. Farnea, R. Isocrate, P. Petkov, N. Marginean, D. Napoli, A. Dewald, *et al.*, Coherent proton-neutron contribution to octupole correlations in the neutron-deficient  $^{114}\text{Xe}$  nucleus, *Phys. Lett. B* **535**, 93 (2002).
- [35] O. Möller, N. Warr, J. Jolie, A. Dewald, A. Fitzler, A. Linnemann, K. O. Zell, P. E. Garrett, and S. W. Yates,  $E2$  transition probabilities in  $^{114}\text{Te}$ : A conundrum, *Phys. Rev. C* **71**, 064324 (2005).
- [36] B. Cederwall, M. Doncel, O. Aktas, A. Ertoprak, R. Liotta, C. Qi, T. Grahn, D. M. Cullen, B. S. Nara Singh, D. Hodge, M. Giles, and S. Stolze, Lifetime measurements of excited states in  $^{172}\text{Pt}$  and the variation of quadrupole transition strength with angular momentum, *Phys. Rev. Lett.* **121**, 022502 (2018).
- [37] T. Bäck, C. Qi, B. Cederwall, R. Liotta, F. Ghazi Moradi, A. Johnson, R. Wyss, and R. Wadsworth, Transition probabilities near  $^{100}\text{Sn}$  and the stability of the  $N, Z = 50$  shell closure, *Phys. Rev. C* **87**, 031306(R) (2013).
- [38] T. Togashi, Y. Tsunoda, T. Otsuka, N. Shimizu, and M. Honma, Novel shape evolution in Sn isotopes from magic numbers 50 to 82, *Phys. Rev. Lett.* **121**, 062501 (2018).
- [39] M. Hjorth-Jensen, T. T. S. Kuo, and E. Osnes, Realistic effective interactions for nuclear systems, *Phys. Rep.* **261**, 126 (1995).

- [40] R. Beck, R. Eder, E. Hagn, and E. Zech, Measurement of the anomalous neutron orbital  $g$  factor in  $^{190m}\text{Os}$ , Phys. Rev. Lett. **59**, 2923 (1987).
- [41] J. M. Allmond, A. E. Stuchbery, A. Galindo-Uribarri, E. Padilla-Rodal, and D. Radford, Investigation into the semimagic nature of the tin isotopes through electromagnetic moments, Phys. Rev. C **92**, 041303(R) (2015).
- [42] P. E. Cavanagh, C. F. Coleman, A. G. Hardacre, G. A. Gard, and J. F. Turner, A study of the nuclear structure of the odd tin isotopes by means of the (p, d) reaction, Nucl. Phys. A **141**, 97 (1970).
- [43] F. Nowacki, Sn calculations in *sdgh* neutron spaces, private communication (2019).
- [44] N. Stone, Table of nuclear electric quadrupole moments, At. Data Nucl. Data Tables **111-112**, 1 (2016).
- [45] T. Tamura and T. Udagawa, Static quadrupole moment of the first  $2^+$  state of vibrational nuclei, Phys. Rev. **150**, 783 (1966).
- [46] P. E. Garrett and J. L. Wood, On the robustness of surface vibrational modes: case studies in the Cd region, J. Phys. G: Nucl. Part. Phys. **37**, 064028 (2010).
- [47] K. Heyde and J. L. Wood, Shape coexistence in atomic nuclei, Rev. Mod. Phys. **83**, 1467 (2011).
- [48] A. Leviatan, N. Gavrielov, J. E. García-Ramos, and P. Van Isacker, Quadrupole phonons in the cadmium isotopes, Phys. Rev. C **98**, 031302(R) (2018).
- [49] P. E. Garrett, T. R. Rodríguez, D. A., K. L. Green, J. Bangay, A. Finlay, *et al.*, Multiple shape coexistence in  $^{110,112}\text{Cd}$ , Phys. Rev. Lett. **123**, 142502 (2019).